Lee et al. Int J Concr Struct Mater (2019) 13:12
https://doi.org/10.1186/s40069-018-0318-8

International Journal of Concrete Structures and Materials

RESEARCH

Open Access

Effect of Recycled Concrete on the Flexural Behavior of Concrete-Filled FRP Tubes

Heeyoung Lee[1,2], Hoon Jang[1] and Wonseok Chung[1*]

Abstract

This paper presents the results of short span concrete-filled fiber reinforced polymer (FRP) tubes filled with different recycled coarse aggregate (RCA) replacement ratios. The mechanical response of recycled concrete-filled FRP tubes (RCFFTs) under flexural load was examined to investigate the influence of RCA as an in-filled material. The experimental results were compared with the simplified finite element model to estimate the failure behavior of the test units. RCFFTs with a 100% RCA replacement ratio showed a similar bending behavior compared to natural aggregate concrete-filled FRP tubes. The flexural behavior of 100% recycled aggregate concrete could be complemented and utilized because of the high strength and high stiffness of the FRPs.

Keywords: concrete-filled, FRP tube, recycled coarse aggregate, FEA

1 Introduction

Construction waste material has gradually increased due to the reconstruction of old deficient structures. In such a situation, it is preferable to use recycled concrete as a structural member to obtain new results and to minimize environmental pollution caused by industrial activities. It has been reported that the compressive strength of concrete constructed with 100% recycled coarse aggregate (RCA) is lower than the compressive strength of normal concrete owing to the high water absorption of RCA (Xiao et al. 2012; Etxeberria et al. 2007). Several experimental studies on the structural behavior and mechanical strength of recycled concrete beams have been performed (1973; Ignjatović et al. 2017; Fathifazl et al. 2011; Silva et al. 2015).

The tension of recycled aggregate concrete must be reinforced by tension carrying material. Fiber reinforced polymers (FRPs) have been extensively considered as an alternative material for tension carrying reinforcement (Lee et al. 2017a, b, c, d). Especially, concrete-filled FRP tubes have been widely investigated as next generation structural members that combine the advantages of FRP and concrete material. The important role of FRP tubes in such a system is to replace steel, while the concrete has a similar role as in general reinforced concrete structures. Additionally, the FRP tubes create shear and flexural reinforced covers, whereas concrete offers good compressive strength and stability for structures against lateral buckling (Mirmiran and Shahawy 1996).

Several researchers have studied circular tubes using FRP (Barbero and Tomblin 1994; Lin et al. 1996; Bambach et al. 2009; Haedir et al. 2009; Lee and Lee 2004; Roberts and Al-Ubaidi 2001; Fam and Son 2008; Shao and Mirmiran 2005, 2007; Fam and Rizkalla 2001; Burgueno and Bhide 2004; Ahmad et al. 2005; Mirmiran et al. 2000; Zhu et al. 2005; Ahmad et al. 2008; Fam and Cole 2007). Significant research efforts have been made to understand concrete-filled FRP tube (CFFT) systems under axial loading or axial-flexural loading (Barbero and Tomblin 1994; Lin et al. 1996; Bambach et al. 2009; Haedir et al. 2009; Lee and Lee 2004; Roberts and Al-Ubaidi 2001). However, a comprehensive review of the literature shows that the behaviors of short span beams have received little attention (Roberts and Al-Ubaidi 2001; Fam and Son 2008; Shao and Mirmiran 2005, 2007; Fam and Rizkalla 2001; Burgueno and Bhide 2004; Ahmad et al. 2005). Short span beams should be considered simultaneously for complex behavior including bending

*Correspondence: wschung@khu.ac.kr
[1] Department of Civil Engineering, College of Engineering, Kyung Hee University, 1732 Deokyoung-Daero, Giheung-Gu, Yongin-Si, Gyeonggi-Do 17104, Republic of Korea
Full list of author information is available at the end of the article
Journal information: ISSN 1976-0485 / eISSN 2234-1315

and shear. In particular, FRP tubes may be at risk of buckling in the case of short spans. Therefore, the structural examination of bending and shear of short span beam FRP tube needs to be studied sufficiently. Mirmiran et al. (2000) observed that beams with a/D ratios (ratio of shear span to outside diameter) of about 2.0 failed in the flexural mode. Zhu et al. (2005) and Ahmad et al. (2008) carried out load tests on ten specimens with a/D ratios between 0.9 and 6.25 and D/t ratios between 16 and 63. It was confirmed that none of the test beams failed in the shear mode. All tested beams failed due to rupture of the FRP tube under longitudinal tension. In addition, short-span concrete-filled FRP beams exhibited higher bending capacity due to the diagonal compression developed in in-filled concrete through arching effects. Fam and Cole (2007) examined the shear behavior of 10 short-span CFFTs reinforced with either steel or FRP longitudinal rebar. All test units failed in terms of the flexure at a/D ratios of about 1. However, all previous research is based on natural aggregate CFFTs. Further experimental and numerical study is necessary to ensure the mechanical behavior of recycled CFFTs under flexural loading.

Several researchers have studied thin-walled circular tubes under bending conditions (Mirmiran et al. 2000; Zhu et al. 2005; Ahmad et al. 2008; Fam and Cole 2007). Some researchers investigated the mechanical behavior of recycled concrete-filled steel tubes (RCFST). Yang and Han (2006) investigated the typical failure modes of RCFST columns with various RCA replacement ratios and found RCFST columns failed due to local buckling, which is the same mechanism as in natural aggregate concrete-filled steel (NCFST) tube columns. The ultimate strength of the 100% RCFST columns is about 10% lower than that for conventional columns. RCFST columns showed better ductility than NCFST columns. Further, RCFST columns have a slightly poorer but generally similar ultimate capacity compared to normal concrete-filled steel tube columns. Wu et al. (2012) and Yang and Ma (2013) investigated the cyclic performances of RCFST columns. Several parameters, including concrete type, axial load ratio, and different sources of demolished concrete, were considered. Huang et al. (2012) developed a theoretical model to predict the mechanical behavior of RCFST under axial compression and obtained that the RCA replacement ratio has a reasonable result on the mechanical behavior of the confined concrete. Most studies on recycled concrete-filled structures are related to steel tube columns. It should be noted that the short span recycled concrete filled FRP tubes (RCFFT) beam has a different load transfer mechanism compared to the relatively long RCFST columns.

Xiao et al. (2012) investigated axial loading tests on recycled concrete columns confined by GFRP material and steel material under axial compressive loading. The key parameters were the recycled coarse aggregate replacement and the type of tube. It was obtained that the maximum stress of RCA confined with GFRP tubes decreases while the corresponding strain increases. Dong et al. (2013) further investigated the structural behavior of RCFST columns wrapped with CFRP. External CFRP wrapping increased the stiffness of RCFST columns significantly due to the restraint on hoop deformations during compressive loading.

No research was found on how the mechanical behavior of RCFFT differs from natural aggregate concrete-filled FRP tubes under bending loads. As the construction industry develops recently, new structures are constructed. A large number of construction and demolition waste aggregates are generated as exist structure is broken down. The interest with recycled materials derived from construction and demolition waste is growing all over the world. Therefore, if recycled aggregate concrete obtained from construction and demolition waste aggregate is used as a structural material, effective construction material circulation can be achieved. Recycled aggregate may be lacking in mechanical performance as a structural material. However, the recycled aggregate can be combined with other materials and exhibit sufficient structural performance. Therefore, this study investigates the effect of structural performance by mixing recycled aggregate in FRP tube. This study investigates the possibility of utilizing recycled concrete as in-filled material for FRP tubes in order to increase the use of recycled materials. The significance of this study lies in extending the application of concrete-filled FRP tubes to the practical uses of RCA. The main objective of this research is to study the mechanical behavior of short span RCFFT beams and to evaluate the structural performance of the proposed system with varying RCA replacement ratios. Several experimental test units are designed and fabricated with varying RCA. The considered RCA replacement ratios are 0%, 25%, 50%, and 100%. The hollow FRP tube alone is also tested to investigate the in-filled effect of concrete as a reference test unit. Five test units were tested under flexural loadings. In addition, simplified finite element analysis (FEA) models of the RCFFT beam are presented and compared with the experimental results.

2 Experimental Program

The experimental program included structural tests of RCFFTs beams under bending loads. A detailed description of the test specimens is provided, including material parameters, fabrication, instrumentation, and test setup. Four RCFFT beams were fabricated with a length of 1100 mm. The outer diameter (D) is 247 mm and the thickness (t) is 5 mm, resulting in an a/D ratio of 1.8 and a D/t ratio of about 50. The reinforcement index, which indicates the amount of reinforcement for the concrete-filled circular tubes as defined in Eq. (1), is calculated to be about 8% (Mirmiran et al. 2000).

$$\rho = \frac{4t}{D} \tag{1}$$

As discussed earlier, the main experimental parameter in this study is the RCA replacement ratio. The RCA replacement ratio was defined as the RCA replacement percentage to the total coarse aggregate by weight. Table 1 shows the details of the test units in the test program. RCFFT-0 is a normal concrete-filled FRP tube while RCFFT-100 is a 100% recycled concrete-filled FRP tube. The hollow FRP tubes were placed in an inclined position and concrete was then placed in the FRP tube. Sufficient vibration was applied to ensure the consolidation of in-filled concrete. All specimens were then air cured for 28 days prior to loading tests. In this study, a hollow FRP tube (HFT) is also prepared to examine the effects of in-filled concrete on the flexural behavior. The material properties of the FRP tube are given as follows. The elastic modulus of the FRP tube is 20 GPa in the axial direction and 21 GPa in the hoop direction. The axial tensile strength is 350 MPa, the axial compressive strength is 340 MPa, and the hoop tensile strength is 200 MPa. A filament winding technique was adopted for fabrication of the cylindrical FRP tube. The process includes winding filaments under variable amounts of tension over a mandrel. The mandrel rotates though a carriage changes horizontally, as shown in Fig. 1, laying down fibers in the desired pattern. The FRP tube consisted of ten-layer laminate with the stacking sequence of $[90_2/\pm 45_3/90_2]$, as shown in Fig. 2a. The orientation of the filaments can also be cautiously organized so that successive layers are supplied or oriented inversely from the prior layer. Figure 1b and c show the fabrication process for lamina orientation at 90° and ± 45°, respectively. The FRP tube was then hardened in a dry oven for 10 h, as shown in Fig. 1d. For in-filled material, ordinary Portland cement (OPC) with a compressive strength of 27.0 MPa was used to fabricate test specimens. Figure 1e shows the prepared aggregate. As discussed earlier, the coarse aggregates are natural coarse aggregates and recycled coarse aggregates (RCA). The ratio of recycled aggregate concrete is shown in Table 1. RCFFT-0 is a mixture of 0% recycled aggregate and RCFFT-25 is 25% recycled aggregate. RCFFT-50 is a specimen mixed with natural aggregate and recycled aggregate by 50%, and RCFFT-100 is a specimen mixed with recycled aggregate only. Samples of 100 × 200 mm concrete cylinders were prepared according to the same RCA replacement ratio as their respective test units (ASTM C 39 2001). During the concrete casting, the compact vibration was performed for the consolidation three times according to the height. Compressive strength tests were carried out using a hydraulic actuator at a constant displacement rate of 1 mm/min. Table 1 shows the compressive strengths of filled concrete. The FRP tube was filled with recycled aggregate concrete, as shown in Fig. 1f.

Table 1 Mix proportions and properties of concrete.

Specimen	RCFFT-0	RCFFT-25	RCFFT-50	RCFFT-100
RCA (kg/m^3)	0	214	427	854
NCA (kg/m^3)	854	640	427	0
Cement (kg/m^3)	354	354	354	354
Sand (kg/m^3)	848	848	848	848
Water (kg/m^3)	202	202	202	202
W/C	57	57	57	57
Compressive strength (MPa)	30.98	29.64	29.60	26.74

RCA recycled coarse aggregate, *NCA* natural coarse aggregate.

Figure 2 shows an overview of the instrumentation and test setup. During a static load test, displacement transducers set up at mid-span and quarter-span to measure deflection. The strain gauges were installed at the bottom surface of the FRP tube in the longitudinal direction to analyze the strain change at each load level. Strain gauges were installed in the hoop direction at the mid-span to test the confining effect at each load level.

The experimental work investigated the load carrying capacity of each specimen as well as failure patterns beyond the ultimate load. The specimens were examined by four-point bending. A vertical servo-controlled hydraulic actuator was located 90 mm apart and at equal distance from the center of the specimen, as shown in Fig. 2a. Because the cross section of the specimen is circular, a half-circular shaped steel frame was attached to the hydraulic actuator, thus supporting the prevention of lateral instability of the specimens, as shown in Fig. 2. The experiment was controlled using the displacement-control method to ensure experimental safety. The load rate was 0.6 mm/min up to failure of the specimens. A data acquisition system was used with a sample rate of 1 Hz.

3 Finite Element Analysis

This study presented the simplified FEA model for recycled concrete-filled FRP tube structures. Rather than applying 3D solid elements as in-filled concrete, 3D fiber beam elements including transverse shear flexibility were used for simplicity. The interface between in-filled concrete and the FRP tube was modeled as rigid links with multi-point constraints. The full composite

a mandrel **b** 90°laminate **c** ±45° laminate **d** hardening **e** preparing the aggregate **f** curing

Fig. 1 Fabrication process for testing.

action was assumed based on the previous experimental results of the short-span CFFT beam (a/D = 2.0, L = 1892 mm) (Ahmad et al. 2008). A comparative slippage between concrete and the FRP tube was measured as approximately 7 mm at failure, which is a very small value compared to the span length. However, a CFFT beam with a/D less than 1.0 showed considerable slippage between concrete and the FRP tubes. Since the test

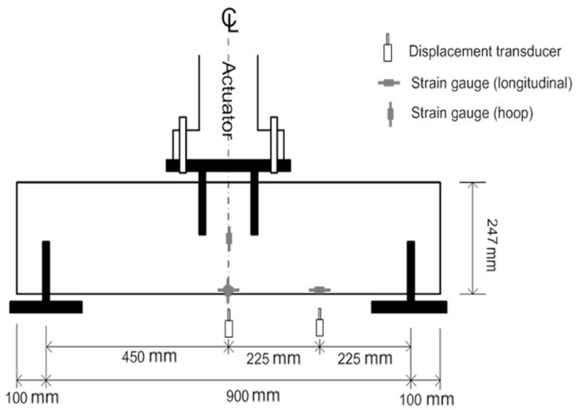

a sensor layout

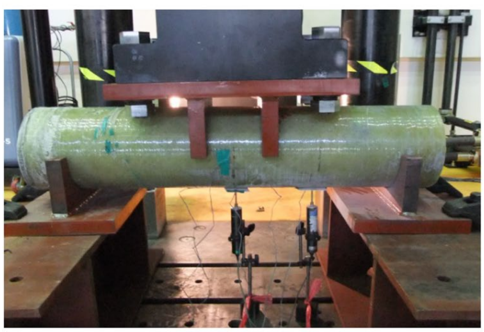

b loading frame

Fig. 2 Test setup.

units have an a/D of 1.8, full composite behavior was assumed and rigid links between concrete beam nodes and FRP shell nodes were applied, as shown in Fig. 3. Analysis was carried out using the non-linear FE analysis program ABAQUS (2007).

For the in-filled concrete in CFFTs, a 3-D three-node Timoshenko Beam element (B32) was used. This B32 element is based on a material model for the uniaxial behavior of concrete based on the work of Hognestad et al. (1956), which studied compression and introduced a smeared crack analogy to explain cracking under tension. Tension stiffening is considered as a descending part in the concrete model to signify the deterioration of cracked concrete sections as the fracture progresses. Figure 4 shows uniaxial concrete model. As concrete exhibits brittle behavior under a tensile load, it is hard to estimate tensile strength (σ_t) correctly, and it is usually expected to be approximately 8% of compressive strength (σ_c). A descending line in this study is used to model this tension stiffening. A smeared model is used to represent the discontinuous crack behavior when cracking of concrete occur. It is recognized that the cracked concrete element can transport the tensile stress in the normal direction to the crack, which is chosen tension stiffening (ASCE Task Committee on Concrete and Masonry Structure 1982). The concrete material is supposed to be initially isotropic, before tensile cracking or compressive yielding. Each element has five fibers per one integration point at which cracking and yielding are checked and the state determination based on material behavior is performed. Cracking occurs when the element's principal stress surpasses the tensile strength of concrete. The element stiffness matrix was informed based on the uniaxial stress–strain relationship defined earlier. An incremental Newton–Raphson iterative procedure is applied to find the equilibrium position at each integration point.

It is noted that the RCA replacement ratio was not considered in the FEA model and the compressive strength of the FEA model was assumed to be 26.74 MPa because FE analysis was conducted to provide a reference for the experimental results and to obtain the structural response of in-filled concrete inside the FRP tube, which is difficult to obtain during testing.

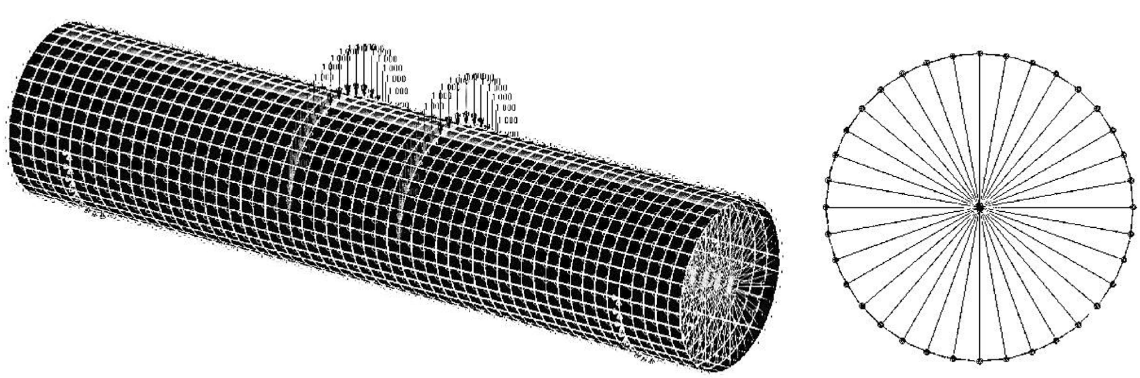

Fig. 3 Finite element model.

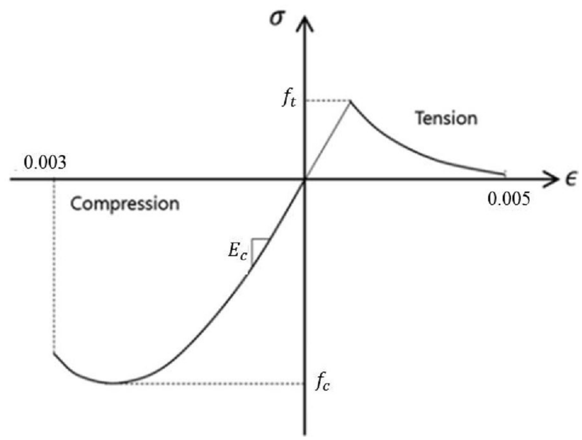

Fig. 4 Uniaxial concrete model.

A quadrilateral shell element was used for the FRP tubes. Numerous ABAQUS-provided shell elements were verified to evaluate their applicability (ABAQUS 2007; Chung and Sotelino 2006). It was obtained that a quadrilateral eight-node shell element with reduced integration (S8R5) predicted the behavior of the thin shell structures. This element was chosen for its displacement compatibility with the concrete beam element. In the ABAQUS implementation, the use of S8R5 elements for FRP tubes and B32 elements for in-filled concrete considers full compatibility between the boundaries of two different elements. The S8R5 element can be used for a layered approach using classical lamination theory. The failure criteria used for the FRP shell were the Tsai–Wu failure criteria. With failure criteria, the Tsai–Wu criterion has been broadly considered in the literature reviews and is implemented in this study. This failure criterion has Eq. (2). The X, Y is the laminate longitudinal in tension and compression, respectively and X′, Y′ is transverse strengths in tension and compression, respectively. S is the shear strength of the lamina.

$$F_1 = \frac{1}{\bar{X}} + \frac{1}{\bar{x'}},\quad F_2 = \frac{1}{\bar{y}} + \frac{1}{\bar{\bar{y'}}},\\ F_{11} = \frac{-1}{\overline{\overline{XX'}}},\quad F_{22} = \frac{-1}{\overline{\overline{YY'}}},\quad F_{66} = \frac{1}{S^2} \tag{2}$$

4 Experimental and Numerical Results

As discussed earlier, RCFFT beams were subjected to 4-point bending and their structural behavior was examined up to failure. This section investigates the effect of the RCA replacement ratio on the strength and failure patterns of RCFFTs. In addition, the influence of in-filled concrete was examined with respect to hollow FRP tubes. In this study, the elastic modulus of concrete (E_c) was calculated as Eq. (3) based on the compressive strength (f_{ck}) according to the ratio of recycled aggregate. The deflection of the specimen was compared with the theoretical deflection (δ) formula. The equation of deflection is given by Eq. (4).

Table 2 Compared load–deflection.

Specimen	Experimental deflection (mm)	Theoretical deflection (mm)	Error rate (%)
HFT	10.70 (at 136.88 kN)	10.42 (at 136.88 kN)	2.6
RCFFT-0	6.32	6.21	1.7
RCFFT-25	6.57	6.33	3.6
RCFFT-50	6.58	6.45	2.0
RCFFT-100	6.86	6.58	4.1

$$E_c = 8500\sqrt[3]{f_{ck} + 8} \tag{3}$$

$$\delta = \frac{PL^3}{48EI} \tag{4}$$

The theoretical deflection calculated by Eq. (4) and the experimental results are compared as shown in Table 2. The deflection error rate of HFT was 2.6% when 136.88 kN loaded. The deflection of all RCFFTs using recycled aggregate concrete resulted in theoretical deflections and a maximum error rate of 4.1% when 150 kN loaded.

According to the load–deflection results given in Table 3, the flexural strength of the concrete-filled FRP beam is significantly higher than that of the hollow FRP beam. The ultimate strength of the HFT specimen was 136.88 kN, while the ultimate strength of the RCFFT specimen composed of RCA was 472 kN, which was about a three-fold strength improvement. That is, RCFFT filled with 100% circulating concrete improved the strength more than 3 times compared to HFT. It was confirmed that the flexural strength of FRP members filled with recycled concrete was improved by restraining the recycled aggregate concrete filled with FRP tubes.

The load–deflection relationship of the HFT specimen is shown in Fig. 5. Figure 8a shows the final failure mode of the HFT. The deflection of the HFT specimen at the ultimate load was 10.7 mm at the top and 4.2 mm at the bottom. There is a difference in deflection between the top and bottom of the fiber. The reason for this is that the HFT is not filled with concrete, and the top surface of the HFT is in direct contact with the actuator, resulting in local displacement. The final upper deflection of the finite element analysis model at the top is 11.85 mm and the final upper deflection of the test results is 10.82 mm. At the bottom, the

Table 3 Load–deflection results.

Load (kN)	HFT (mm)	RCFFT-0 (mm)	RCFFT-25 (mm)	RCFFT-50 (mm)	RCFFT-100 (mm)
150	10.70 (at 136.88 kN)	6.32	6.57	6.58	6.86
250	–	11.01	11.24	11.26	12.00
350	–	15.90	16.66	17.01	17.59
450	–	21.60	23.07	23.38	23.85

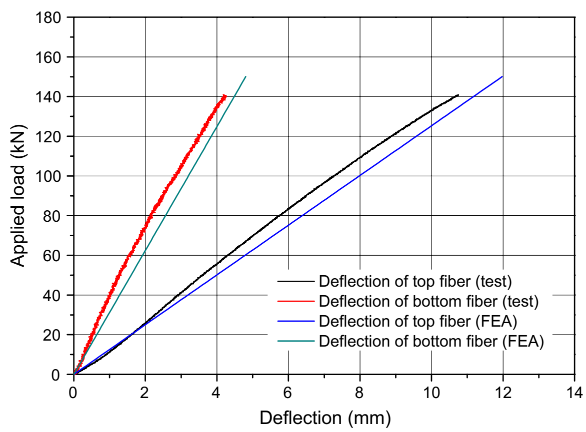

Fig. 5 Load–deflection response of HFTs.

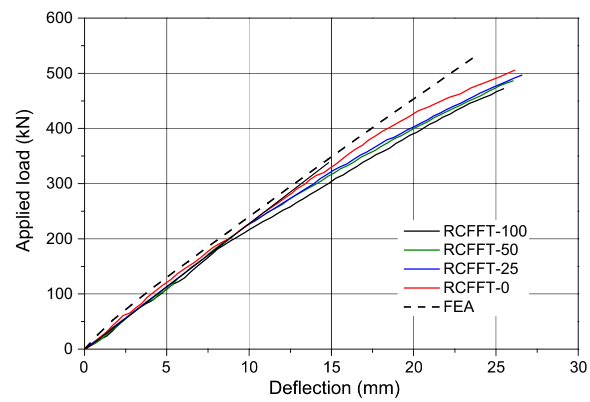

Fig. 6 Load–deflection response of RCFFTs at mid-span.

final deflection of the finite element analysis model is 4.74 mm and the final deflection of the test results is 4.23 mm. Both the finite element analysis and the experimental results behaved similarly with error rates within 10%.

The experimental load–deflection response at the mid-span and at the quarter-span of the RCFFT beams are plotted with the FEA results in Figs. 6 and 7, respectively. It is observed that both the experimental and FEA results were slightly nonlinear up to failure. At the mid-span, the test results exhibited linear behavior when the applied load was about 200 kN, while FEA results were linear up to when the first cracking was detected at the bottom fiber of the concrete element. Later, a slight non-linear behavior was exhibited due to the progressive cracking of in-filled concrete with increasing load. The final failure occurred when the test beam exhibited flexural cracking and the mid-span yielded. However, it is studied that the FEA results were slightly stiffer than the experimental results. This difference might happen as in the FEA model, the interface of concrete and FRP tube were modeled to have full composite behaviors up to their failure state by using rigid links. The final ultimate load of FEA for RCFFT-0 was 530 kN, representing a 4.7% difference from the experimental results (506 kN). Similar trends were observed at the quarter-span, as shown in Fig. 7. The deflections predicted using the simplified FEA models have been compared to those obtained from the experiments. Generally, suitable results were obtained, given the complex nature of local buckling failure of circular hollow tubes under bending.

All test specimens failed in a brittle manner. The failure mode for RCFFP-0 is shown in Fig. 8b. All test beams failed in flexural mode regardless of the RCA ratio. The failure mode implied that tensile strains at the bottom of the mid-span were larger than the diagonal tensile strain at the mid-span. FRP tubes filled with recycled aggregate concrete and normal concrete all failed due to FRP rupture in the extreme tensile fiber, which is typical of tension-dominated flexural failure. In the mid-span of the FRP tube, tensile stresses exceeding the rupture strain of FRP occurred. Tensile rupture of FRP tube starts in the most highly stressed FRP tube. It is observed that all test specimens exhibited highly localized flexural cracks under the loading points. Once flexural cracks progress, they tend to quickly run through the whole depth of in-filled concrete, resulting in splitting of the test unit in half.

The flexural strengths of RCFFTs are plotted against different RCA replacement ratios in Fig. 9. In general,

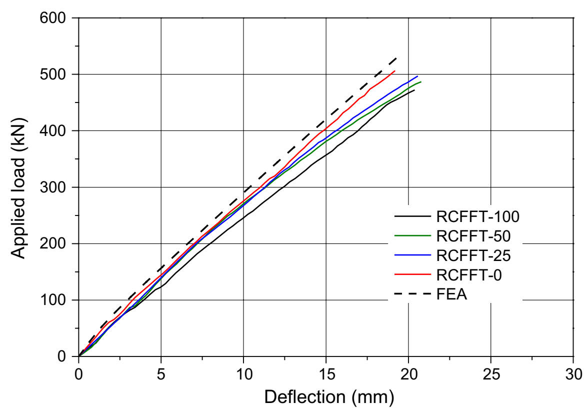

Fig. 7 Load–deflection response of RCFFTs at quarter span.

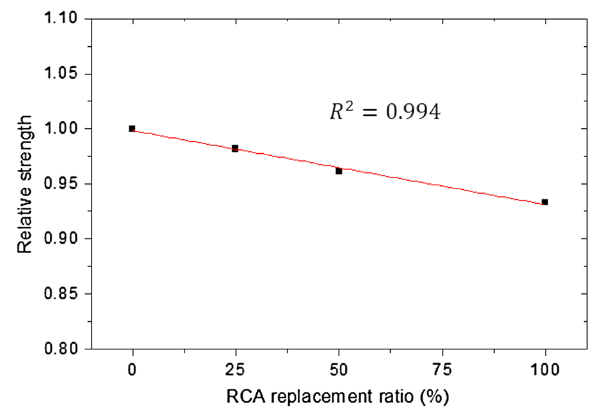

Fig. 9 Influence of RCA content on ultimate strength.

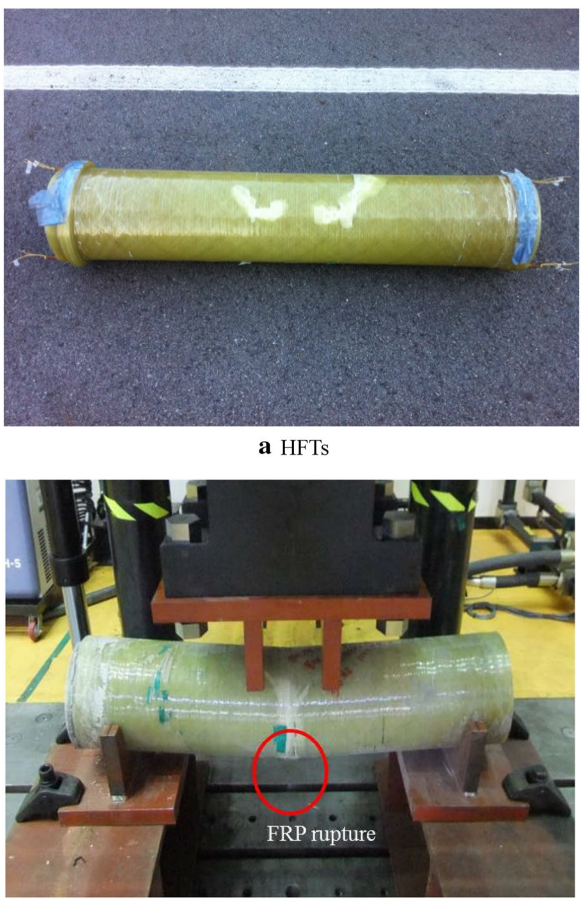

a HFTs

b RCFFTs

Fig. 8 Failure mode.

specimens with natural aggregate-filled concrete result in higher ultimate strength compared to specimens with RCA-filled specimens. It is clearly observed that the strength steadily decreased as the RCA replacement ratio increased. The regression coefficient was 0.994 for the test units. The strength of RCFFT-0 is higher than the strengths of RCFFT-100 and RCFFT-50 by 6.7% and 3.8%, respectively. Based on the linear regression apparent in the test results, the relative strength (S) can be estimated as a formula of the RCA replacement ratio as

$$S = -0.0007\text{RCA}(\%) + 1.0. \quad (5)$$

According to the compressive strength of the recycled concrete cylinder given in Table 1, the compressive strength of the natural concrete cylinder was 31.0 MPa while that of all recycled concrete was 26.7 MPa, a 16% difference. However, the strength of the CFFTs with all natural aggregate concrete is more than 6.7% higher compared to the CFFTs with all RCA. This indicates that the structural weakness of recycled concrete was reinforced by FRP material. Thus, recycled concrete can be applied as in-filled material for future construction.

Figure 10a shows the strain results of FRP in the longitudinal and circumferential directions at the mid-span. From the strain results in the longitudinal direction, it could be observed that the maximum tensile stress is generated in the lower part of the FRP of the mid-span. As the load increases, the tensile stress of FRP at L/4 increased. The tensile strains at the bottom fiber of the mid-span were larger than the diagonal tensile strain at the mid-span. Figure 10b presents numerical prediction of circumferential strains of the bottom fiber at mid-span. At the final load, the circumferential strain of the FEA model was 3046 με, and the circumferential strain of the test results was 3308 με. The FEA model and the experimental results have 8.6% error, but the FEA model predicts the results extremely well for all cases.

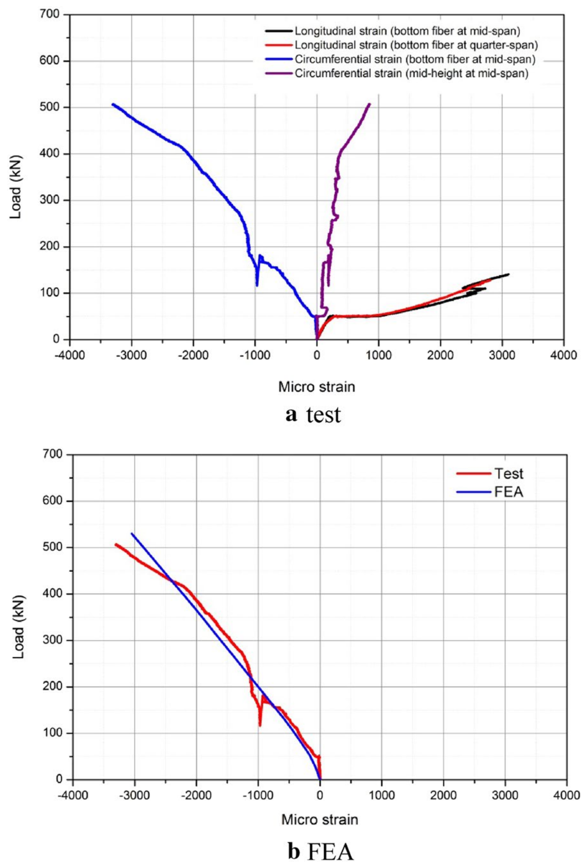

Fig. 10 Load–strain response.

5 Conclusions

In this study, RCFFT specimens were fabricated and tested with different recycled coarse aggregate ratios to examine flexural behavior. This study also presents simplified finite element models. The following conclusions were obtained in this study.

1. The flexural strength of RCFFTs is significantly higher than that of a hollow FRP beams. RCFFTs filled using 100% recycle concrete improved the strength more than 3 times compared with HFT. It is confirmed that the FRP specimen filled with the recycled aggregate concrete significantly improved the flexural strength by restraining the recycled aggregate concrete filled with the FRP tube.
2. The flexural strength of the CFFTs with all RCA is 6.7% lower compared to CFFTs with all natural aggregate concrete. It was confirmed that the structural performance of recycled aggregate concrete could be complemented and utilized because of the high strength and high stiffness of the FRPs.
3. As the load increased, the FRPs filled with the recycled aggregate concrete proceeded to fracture as the initial cracks formed in the filled concrete. As the cracks in the inner concrete progressed, the strain rapidly increased in the lower part of the mid-span of the FRP. The final failure mode was brittle fracture as the fibers of the FRP tube were locally fractured.
4. The proposed finite element model in this study can predict the load level and circumferential deformation. The proposed FEA model predicted behavior similar to the experimental failure mode.

Authors' contributions

HL studied the experimental results on this page and proposed a finite element analysis model. HJ performed compressive strength tests and flexural tests and analyzed the experimental results. WC managed this paper collectively. All authors read and approved the final manuscript.

Author details

[1] Department of Civil Engineering, College of Engineering, Kyung Hee University, 1732 Deokyoung-Daero, Giheung-Gu, Yongin-Si, Gyeonggi-Do 17104, Republic of Korea. [2] Department of Civil Engineering, University of Colorado Denver, 1200 Larimer Street, Denver, CO 80217, USA.

Acknowledgements

This research was supported by a grant (2017R1A2B4010467 and 2017R1C1B1006732) from the National Research Foundation of Korea through Ministry of Science, ICT and Future Planning, South Korea.

Competing interests

The authors declare that they have no competing interests.

Availability of data and materials

Not applicable.

Funding

This study is a basic research project conducted with support from the National Research Foundation of Korea through government funds (Ministry of Science, ICT and Future Planning, South Korea). The Project Numbers are 2017R1A2B4010467 and 2017R1C1B1006732.

Publisher's Note

Received: 15 January 2018 Accepted: 11 November 2018
Published online: 28 January 2019

References

ABAQUS. (2007). *ABAQUS/Standard User's Manual. Version 6.71*. Pawtucket: ABAQUS Inc.

Ahmad, I., Zhu, Z., & Mirmiran, A. (2008). Behavior of short and deep beams made of concrete-filled fiber-reinforced polymer tubes. *Journal of Composites for Construction, 12*(1), 102–110.

Ahmad, I., Zhu, Z., Mirmiran, A., & Fam, A. (2005). *Shear strength prediction of deep CFFT beams. Fiber reinforced polymers (FRP) for reinforced concrete structures, VII,* 1085–1102.

ASCE Task Committee on Concrete and Masonry Structure. (1982). *State of the art report on finite element analysis of reinforced concrete*. New York: ASCE.

ASTM C 39. (2001). *Standard test method for compressive strength of cylindrical concrete specimens*. New York: ASTM International.

Bambach, M. R., Jama, H. H., & Elchalakani, M. (2009). Axial capacity and design of thin-walled steel SHS strengthened with CFRP. *Thin-Walled Structures, 47*(10), 1112–1121.
Barbero, E., & Tomblin, J. (1994). A phenomenological design equation for FRP columns with interaction between local and global buckling. *Thin-Walled Structures, 18*(2), 117–131.
Buck, A. D. (1973). *Recycled concrete highway res record* (pp. 1–8). Washington, D.C: Highway Research Board.
Burgueno, R., Bhide, K. (2004) Shear stresses in concrete-filled FRP cylindrical shells in bending. In *Proceedings of the 4th advanced composite materials in bridges and structures*, Canada, Calgary (pp. 1–8).
Chung, W., & Sotelino, E. D. (2006). Three-dimensional finite element modeling of composite girder bridges. *Engineering Structures, 28*(1), 63–71.
Dong, J. F., Wang, Q. Y., & Guan, Z. W. (2013). Structural behaviour of recycled aggregate concrete filled steel tube columns strengthened by CFRP. *Engineering Structures, 48,* 532–542.
Etxeberria, M., Vázquez, E., Marí, A., & Barra, M. (2007). Influence of amount of recycled coarse aggregates and production process on properties of recycled aggregate concrete. *Cement and Concrete Research, 37*(5), 735–742.
Fam, A., & Cole, B. (2007). Tests on reinforced-concrete-filled, fiber-reinforced-polymer circular tubes of different shear spans. *Canadian Journal of Civil Engineering, 34*(3), 311–322.
Fam, A. Z., & Rizkalla, S. H. (2001). Confinement model for axially loaded concrete confined by circular fiber-reinforced polymer tubes. *Structural Journal, 98*(4), 451–461.
Fam, A., & Son, J. K. (2008). Finite element modeling of hollow and concrete-filled fiber composite tubes in flexure: Optimization of partial filling and a design method for poles. *Engineering Structures, 30*(10), 2667–2676.
Fathifazl, G., Razaqpur, A. G., Isgor, O. B., Abbas, A., Fournier, B., & Foo, S. (2011). Shear capacity evaluation of steel reinforced recycled concrete (RRC) beams. *Engineering Structures, 33*(3), 1025–1033.
Haedir, J., Bambach, M. R., Zhao, X. L., & Grzebieta, R. H. (2009). Strength of circular hollow sections (CHS) tubular beams externally reinforced by carbon FRP sheets in pure bending. *Thin-Walled Structures, 47*(10), 1136–1147.
Hognestad, E. (1956). *Ultimate strength of reinforced concrete in American design practice*. New York: Portland Cement Association, Research and Development Laboratories.
Huang, Y., Xiao, J., & Zhang, C. (2012). Theoretical study on mechanical behavior of steel confined recycled aggregate concrete. *Journal of Constructional Steel Research, 76,* 100–111.
Ignjatović, Ivan S., Marinković, Snežana B., & Tošić, Nikola. (2017). Shear behaviour of recycled aggregate concrete beams with and without shear reinforcement. *Engineering Structures, 141,* 386–401.
Lee, H., Jung, W. T., & Chung, W. (2017a). Bond behavior of near surface mounted CFRP rods under temperature cycling. *Engineering Structures, 137,* 67–75.
Lee, H., Jung, W. T., & Chung, W. (2017b). Flexural strengthening of reinforced concrete beams with pre-stressed near surface mounted CFRP systems. *Composite Structures, 163,* 1–12.
Lee, H., Jung, W. T., & Chung, W. (2017c). Post-tension near-surface-mounted strengthening systems of full-scale PSC girders. *Construction and Building Materials, 151,* 71–82.
Lee, H., Lee, W., Jung, W. T., & Chung, W. (2017d). Bond characteristics of near-surface-mounted anchorage for prestressing. *Construction and Building Materials, 148,* 748–756.
Lee, J., & Lee, S. (2004). Flexural–torsional behavior of thin-walled composite beams. *Thin-Walled Structures, 42*(9), 1293–1305.
Lin, Z. M., Polyzois, D., & Shah, A. (1996). Stability of thin-walled pultruded structural members by the finite element method. *Thin-Walled Structures, 24*(1), 1–18.
Mirmiran, A., & Shahawy, M. (1996). A new concrete-filled hollow FRP composite column. *Composites Part B Engineering, 27*(3–4), 263–268.
Mirmiran, A., Shahawy, M., Khoury, C. E., & Naguib, W. (2000). Large beam-column tests on concrete-filled composite tubes. *ACI Structural Journal, 97*(2), 268–276.
Roberts, T. M., & Al-Ubaidi, H. (2001). Influence of shear deformation on restrained torsional warping of pultruded FRP bars of open cross-section. *Thin-Walled Structures, 39*(5), 395–414.
Shao, Y., & Mirmiran, A. (2005). Experimental investigation of cyclic behavior of concrete-filled fiber reinforced polymer tubes. *Journal of Composites for Construction, 9*(3), 263–273.
Shao, Y., & Mirmiran, A. (2007). Control of plastic shrinkage cracking of concrete with carbon fiber-reinforced polymer grids. *Journal of Materials in Civil Engineering, 19*(5), 441–444.
Silva, R. V., De Brito, J., & Dhir, R. K. (2015). Comparative analysis of existing prediction models on the creep behaviour of recycled aggregate concrete. *Engineering Structures, 100,* 31–42.
Wu, B., Zhao, X. Y., & Zhang, J. S. (2012). Cyclic behavior of thin-walled square steel tubular columns filled with demolished concrete lumps and fresh concrete. *Journal of Constructional Steel Research, 77,* 69–81.
Xiao, J., Huang, Y., Yang, J., & Zhang, C. (2012). Mechanical properties of confined recycled aggregate concrete under axial compression. *Construction and Building Materials, 26*(1), 591–603.
Yang, Y. F., & Han, L. H. (2006). Experimental behaviour of recycled aggregate concrete filled steel tubular columns. *Journal of Constructional Steel Research, 62*(12), 1310–1324.
Yang, Y. F., & Ma, G. L. (2013). Experimental behaviour of recycled aggregate concrete filled stainless steel tube stub columns and beams. *Thin-Walled Structures, 66,* 62–75.
Zhu, Z., Ahmad, I., & Mirmiran, A. (2005). Effect of column parameters on axial compression behavior of concrete-filled FRP tubes. *Advances in Structural Engineering, 8*(4), 443–449.